BIOLOGY OF REPRODUCTION (2013) **89**(4):94, 1–10
Published online before print 4 September 2013.
DOI 10.1095/biolreprod.113.111963

Quantified Colocalization Reveals Heterotypic Histocompatibility Class I Antigen Associations on Trophoblast Cell Membranes: Relevance for Human Pregnancy[1]

Asma Jabeen,[3] José Maria Miranda-Sayago,[3] Boguslaw Obara,[4] Patrick Simon Spencer,[3] Gill Barbara Dealtry,[5] Soren Hayrabedyan,[6] Valerie Shaikly,[7] Pierre Philippe Laissue,[3] and Nelson Fernández[2,3]

[3]*School of Biological Sciences, University of Essex, Colchester, United Kingdom*
[4]*Engineering and Computing Sciences, University of Durham, Durham, United Kingdom*
[5]*Department of Biochemistry and Microbiology, Nelson Mandela Metropolitan University, Summerstrand South Campus, South Africa*
[6]*Institute of Biology and Immunology of Reproduction, Sofia, Bulgaria*
[7]*Assisted Reproduction and Gynecology Centre, London, United Kingdom*

ABSTRACT

Human placental syncytiotrophoblasts lack expression of most types of human leukocyte antigen (HLA) class I and class II molecules; this is thought to contribute to a successful pregnancy. However, the HLA class Ib antigens HLA-G, -E, and -F and the HLA class Ia antigen HLA-C are selectively expressed on extravillous trophoblast cells, and they are thought to play a major role in controlling feto-maternal tolerance. We have hypothesized that selective expression, coupled with the preferential physical association of pairs of HLA molecules, contribute to the function of HLA at the feto-maternal interface and the maternal recognition of the fetus. We have developed a unique analytical model that allows detection and quantification of the heterotypic physical associations of HLA class I molecules expressed on the membrane of human trophoblast choriocarcinoma cells, ACH-3P and JEG-3. Automated image analysis was used to estimate the degree of overlap of HLA molecules labeled with different fluorochromes. This approach yields an accurate measurement of the degree of colocalization. In both JEG-3 and ACH-3P cells, HLA-C, -E, and -G were detected on the cell membrane, while the expression of HLA-F was restricted to the cytoplasm. Progesterone treatment alone induced a significant increase in the expression level of the HLA-G/HLA-E association, suggesting that this heterotypic association is modulated by this hormone. Our data shows that the cell-surface HLA class I molecules HLA-G, -E, and -C colocalize with each other and have the potential to form preferential heterotypic associations.

bioimaging, bioinformatics, immunology, implantation, MHC class I, pregnancy, progesterone, trophoblasts

INTRODUCTION

In mammals, the proteins encoded by the major histocompatibility complex (MHC) play a key role in adaptive immunity and reproduction. In human pregnancy, at the feto-maternal interface, the pattern of MHC protein expression on placental trophoblast cells differs from that on other somatic cell types. Syncytiotrophoblasts, the cells that cover the chorionic villi, which are in direct contact with maternal blood, lack expression of most types of human leukocyte antigen (HLA) class I and class II molecules. This minimizes antigen presentation events as well as a local inflammatory reaction, which otherwise would compromise pregnancy. In contrast, the extravillous trophoblast (EVT) population, which penetrates into the decidualized uterus, expresses the polymorphic classical class Ia molecule HLA-C, mainly during the first trimester of pregnancy [1], and also the nonclassical class Ib HLA-G [2–4], HLA-E [5], and HLA-F [6]. The complete absence of HLA class II molecules and the class Ia molecules HLA-A and -B in trophoblast cells, and the expression of HLA-C during the first trimester, coupled with high levels of HLA-G, -E, and -F throughout gestation, are probably the result of strong directional selection in favor of fetal tolerance by the maternal immune system [6, 7].

The HLA-C molecule is found intracellularly and on the surface of normal human first-trimester EVT. Cell surface levels of HLA-C are 10-fold lower than those of HLA-A and -B. In contrast to HLA-A and -B, the peptide-binding groove of HLA-C is less polymorphic, and its β-2 microglobulin (β-2m)-free heavy chains are better stabilized on the cell surface [1]. HLA-C, together with the HLA class Ib molecules HLA-G, -E, and -F, might play a functional role in natural killer (NK) cell recognition and in achieving optimal allograft protection during pregnancy. Total loss of HLA-A and -B at the cell surface increases susceptibility to NK cell-mediated lysis [8].

In human pregnancy, the expression of HLA-G is restricted to fetal trophoblast tissue [3]. In contrast, HLA-E is expressed on most cells that also express other HLA class I molecules, including trophoblasts [6]. HLA-G primary transcript is alternatively spliced to produce seven mRNAs that encode four membrane-bound (HLA-G1, -G2, -G3, and -G4) and three soluble (HLA-G5, -G6, and -G7) protein isoforms [9–12]. Membrane-bound HLA-G has been associated with the inhibition of uterine NK (uNK) and T-cell cytolysis [13]. HLA-E depends on its interaction with a restricted set of nonamer peptides derived from the leader sequence of other HLA class I molecules [14], suggesting that for cell surface expression, an association of HLA-E with other Class I molecules is required.

HLA-F was initially reported to be retained intracellularly [15, 16]. However, cell surface expression has been shown on some B lymphocyte and monocytic cell lines where, unlike other class I molecules, cell surface expression is partially independent of tapasin and completely independent of TAP

[1]Supported by the University of Essex and the Assisted Reproduction Gynecology Centre (London) United Kingdom
[2]Correspondence: Nelson Fernández, School of Biological Sciences, University of Essex, Wivenhoe Park, Colchester, CO4 3SQ, United Kingdom. E-mail: nelson@essex.ac.uk

Received: 3 July 2013.
First decision: 2 August 2013.
Accepted: 29 August 2013.

eISSN: 1529-7268 http://www.biolreprod.org
ISSN: 0006-3363

transporters [17]. HLA-F surface expression has also been demonstrated on EVT in normal term placenta [6].

We have employed a high-precision single-cell bioimaging protocol and quantified the formation of HLA heterotypic molecules. Detecting and quantifying the associations of proteins using microscopy is limited by the fact that visible light is diffracted. This phenomenon limits the resolving power of a fluorescence microscope to 200–350 nm. A single, fluorescently tagged protein will appear as a diffraction-limited spot, blurred and around 10 times larger than its actual size. The center, from which all light of the blurred spot emanates, can be calculated with a precision far higher than the diffraction limit [18]. This technique permits the estimation of the molecular position of the tagged protein with certain accuracy [19–23]. The technique enables the localization of single fluorophores with a precision ranging from 40 nm to the subnanometer scale [24–26], and it is fundamental to recent superresolution microscopy techniques such as STORM and PALM (for review, see, e.g., [27]). If two different kinds of molecules are labeled with different colors, their closeness can be assessed with similar precision. We have previously developed an approach for studying such subdiffraction-limited colocalization [28]. Here, we apply our most recent method [29]. It allows for the determination of the proximity of two different cell surface receptors, based on histograms derived from their localization measurements. We hypothesize that the selective expression of HLA class I antigens, coupled with the preferential physical association of pairs of HLA molecules, contributes to immunotolerance and the function of HLA at the feto-maternal interface.

MATERIALS AND METHODS

Cell Lines and Cell Culture

The JEG-3 and the novel ACH-3P trophoblast hybrid cell lines were used. The ACH-3P cell line was kindly provided by Dr. G. Desoye (Department of Obstetrics and Gynecology, Medical University of Graz, Graz, Austria). This cell line was established by fusion of primary human first-trimester trophoblasts with a human choriocarcinoma cell line (AC1-1) [30] and culture in Ham F-12 with stable glutamine medium, supplemented with 10% (v/v) fetal bovine serum (FBS). The JEG-3 cell line (kindly provided by Professor I.L. Sargent, Nuffield Department of Obstetrics and Gynecology, University of Oxford, Oxford, U.K.) was maintained in Dulbecco modified Eagle medium/Ham F-12 containing 10% (v/v) FBS. All media and sera were purchased from PAA Laboratories GmbH (Pasching, Austria). Both cell lines were cultured in a humidified atmosphere of 5% CO_2 at 37°C.

Anti-HLA-Class I Monoclonal Antibodies

The following HLA class I-specific primary monoclonal antibodies were used. Anti-HLA-G-specific MEM-G/09 reacts exclusively with native HLA-G1 molecules and was previously defined for flow cytometry and immunohistochemistry (IHC) staining. The MEM-G/01 clone that recognizes the denatured HLA-G heavy chain of all isoforms is used for Western blotting. Anti-HLA-E-specific MEM-E/02 reacts specifically with denatured HLA-E molecules and is employed for Western blotting, whereas MEM-E/07 recognizes native surface HLA-E molecules and is used for fluorescence-activated cell sorting (FACS) analysis and IHC staining. Specificity of HLA-G and -E antibodies was previously thoroughly validated by flow cytometry at the Third International Conference on HLA-G (Paris, July 2003) [31] and by separate validation studies [32, 33]. The HLA-C-specific antibody L31 is known to bind to an epitope present on all HLA-C alleles (CW1 through CW8) and cross-reacts with HLA-B alleles (HLA-B7, -B8,-B35, -B51, and others) [34]. Anti-HLA-F (3D11) recognizes native and denatured forms of HLA-F and does not cross-react with any other HLA type [6]. MEM-G/09 (IgG1; EXBIO Praha, Vestec, Czech Republic) is here used for FACS analysis and confocal microscopy. MEM-G/01 (IgG1; EXBIO Praha) was used for Western blotting. MEM-E/07 (IgG1; EXBIO Praha), used for FACS and confocal microscopy, is known to cross-react with the classical MHC class I molecules HLA-B7, -B8, -B27, and -B44, whereas MEM-E/02 (IgG1; EXBIO Praha) is used for Western blotting and does not cross-react with HLA-A, -B, -C, or -G [35]. L31 (IgG1; Media Pharma, Chieti, Italy) was employed for FACS and confocal microscopy, while anti-HLA-C clone D-9 (BioLegend, San Diego, CA) was used for Western blotting. The HLA-F-specific clone 3D11 (IgG1; kindly provided by Dr. Daniel Geraghty, Seattle, WA) was used for FACS, confocal microscopy, and Western blotting.

Flow Cytometry Analysis

Cell cultures were washed twice with PBS and incubated with Accutase (PAA Laboratories GmbH) for 7–10 min at 37°C. Cell suspensions (1×10^6 cells per sample) were centrifuged at $300 \times g$ for 10 min. Supernatants were discarded, and the cell pellets were resuspended in blocking buffer (PBS supplemented with 0.1% [w/v] bovine serum albumin [BSA]). The cells were incubated at 4°C for 1 h with saturating concentrations of the following primary human specific monoclonal antibodies: anti-HLA-G clone MEM-G/09, anti-HLA-E clone MEM-E/07, anti-HLA-C clone L31, and anti-HLA-F clone 3D11. The cells were washed twice with PBS, and bound primary monoclonal antibody was detected with fluorescein isothiocyanate (FITC)-conjugated goat anti-mouse IgG (Santa Cruz Biotechnologies Inc., Santa Cruz, CA). A minimum of 10 000 events were acquired for each sample using a BD FACS Calibur equipped with BD CellQuest software (Becton Dickinson, San Diego, CA). The results were analyzed using FlowJo version 8.8.6 (Tree Star Inc., Ashland, OR).

Cell Surface Antigen Quantification

Cell surface antigen quantification was performed using Qifikit beads (Dako A/S, Glostrup, Denmark) as described previously [36]. Briefly, cell samples were prepared as for the flow cytometry analysis up to the step of primary antibody binding. For detection of antibody staining, the cell samples, setup beads, and calibration beads were stained with FITC-conjugated secondary antibody provided with the kit. The system was calibrated for the cell isotype and setup beads. Using the same settings, data for cell samples and calibration beads were acquired. A calibration curve was constructed for mean fluorescence intensity and each population of beads. The antigen-binding capacity of cells was calculated by interpolation on the calibration curve. Surface antigens were quantified by determining the ratio of antibody bound to cells relative to the calibration beads. Antibody titrations were performed for all the antibodies on both cell lines under study to ensure that all the surface molecules were detected.

Western Blotting and Immunodetection

Cells were lysed with CelLytic MT reagent (Sigma-Aldrich, St. Louis, MO), and total protein concentration was determined by the Bio-Rad Protein Assay (Bio-Rad, Hercules, CA) following the manufacturer's instructions. The total cell lysate was separated on a 12% (w/v) SDS-PAGE gel. A total of 40 μg of protein was loaded per well, and after electrophoresis, protein was transferred to a polyvinylidene fluoride membrane (Immobilon-FL; Merck Millipore, Merck KGaA, Darmstadt, Germany). Membranes were blocked with 5% (w/v) skimmed milk in PBS. The following monoclonal antibodies were used to detect HLA class I proteins: anti-HLA-C (clone D-9), anti-HLA-F (clone 3D11), anti-HLA-E (clone MEM-E/02), and anti-HLA-G (clone MEM-G/01). An alpha subunit-specific tubulin mouse monoclonal antibody was used to probe the cell extracts and loaded as a control (Biolegend). The IRDye 800CW Donkey Anti-Mouse IgG (Li-Cor Biosciences, Lincoln, NE) was used as the secondary antibody at a dilution of 1:10 000 in PBS with 5% (w/v) milk and 0.025% (v/v) Tween-20 (Sigma-Aldrich). Signals were detected using the ODYSSEY infrared imaging system (Li-Cor Bioscience). To estimate the molecular weight of the proteins under study, the Fermentas PulerageR Plus Prestained Protein Ladder (Thermo Fisher Scientific, Waltham, MA) was used.

Immunofluorescence Staining for Bioimaging Analysis

ACH-3P and JEG-3 cells were seeded on LabTek eight-well slides (Thermo Fisher Scientific) at a density of 8×10^3 cells per well and cultured for 2 days. Cells were serum starved overnight and the next day treated with or without 1 μg/ml of progesterone (PG; Sigma-Aldrich) with low serum (0.1% [v/v] FBS) for 24 h. The cells were then fixed with 4% (w/v) paraformaldehyde on ice for 20 min. All subsequent steps were carried out at room temperature unless stated otherwise. Cells were blocked with 2% (w/v) BSA in PBS for 1 h. Staining was done sequentially for each antigen. The cells were incubated with the following primary anti-human monoclonal antibodies: anti-HLA-G (clone MEM-G/09) and anti-HLA-E (clone MEM-E/07) at a dilution of 2 μg/100 μl in PBS for 1 h; anti-HLA-C (clone L31) and anti-HLA-F (clone 3D11) at a dilution of 1 μg/100 μl in PBS for 1 h. The samples were washed three times with PBS and

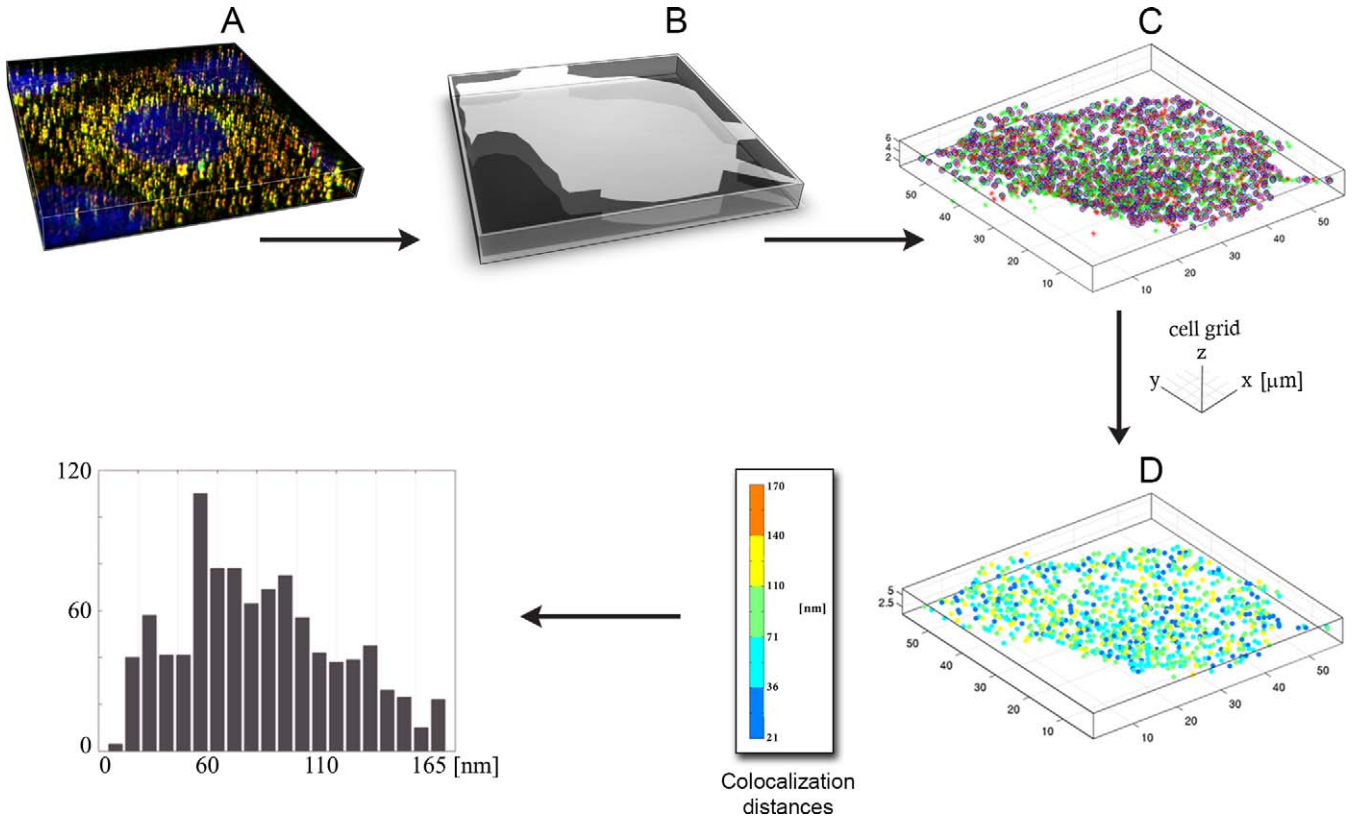

FIG. 1. Colocalization detection and quantification of HLA receptors on the cell surface of human trophoblast-derived choriocarcinoma cells. **A**) 3D image of a JEG-3 cell showing blue (nucleus), green (HLA-E), red (HLA-C), and yellow/orange potentially colocalized particles. **B**) Mask image of single cell (gray) shown in **A**. Cell outline was traced using differential interference contrast and its fluorescence image. **C**) 3D scatter plot of a single cell depicting the relationship between HLA-E (green asterisks) and HLA-C (red asterisks). Blue circles designate colocalized HLA-E and -C molecules. Total number of red, green, and colocalized spots per cell is quantified. **D**) Color-coded 3D scatter plot for Euclidean distance map of colocalized particles. The color scale indicates the distance between the centroids of colocalized pairs ranging from 10–165 nm (colocalization distance threshold $d = 165$ nm). The corresponding histogram represents colocalization distance on the *x*-axis and the number of colocalizations on the *y*-axis. Note that the grid for cellular dimensions uses micrometers.

incubated for 1 h with anti-mouse IgG antibody conjugated with Alexa Fluor 488 or Alexa Fluor 555 (Invitrogen, Carlsbad, CA) at a dilution of 0.25 µg/100 µl. For staining cell nuclei, 4′,6-diamidino-2-phenylindole (DAPI; Sigma-Aldrich) was used at a 1:250 dilution in PBS. The cells were thoroughly washed thereafter and air dried. The slides were mounted with Vectashield mounting medium (Vector Laboratories, Burlingame, CA), covered with cover slips, and sealed with Marabu Fixogum rubber cement (Marabuwerke GmbH & Co. KG, Tamm, Germany).

Confocal Microscopy

For image acquisition, a Nikon A1si laser scanning confocal microscope was used with a plan-apochromatic, violet-corrected, 60× magnifying, 1.4-numerical aperture (N.A.) oil-immersion objective and NIS Elements software version 3.21.03 (Nikon, Tokyo, Japan). Three-dimensional (3D) single-cell images were acquired in four channels for DAPI (excitation at 405 nm with laser power 3.2 arbitrary units [AU], emission collection at 450/50 nm, and photomultiplier tube [PMT] gain 118 AU), Alexa Fluor 488 (excitation 488 nm with laser power 7.8 AU, emission collection at 525/50 nm, and PMT gain 140 AU; called green channel), Alexa Fluor 555 (excitation 561 nm with laser power 2.1 AU, emission collection at 595/50 nm, and PMT gain 117 AU; called red channel), and differential interference contrast (DIC; transmitted light detector gain 103 AU) using one-way sequential line scans (Fig. 1A). All the images were acquired with the same settings for the microscope where scan speed was 1/4 frames (galvano scanner), and no offset was used. The pinhole size was 34.5 µm, approximating 1.2 times the Airy disk size of the 1.4 N.A. objective at 525 nm. Scanner zoom was centered on the optical axis and set to a lateral magnification of 55 nm/pixel and a Nyquist factor of 2.54 (for Alexa Fluor 488) and 2.79 (for Alexa Fluor 555). Axial step size was 140 nm, with 40–60 image planes per z-stack.

Image Preprocessing

Acquired 3D images were processed for alignment and deconvolution before analysis. In some data sets, stage drift was observed. Image stacks were, thus, aligned using the translational mode of the StackReg algorithm [37] in ImageJ [38]. Deconvolution of images was performed using Autoquant X software version 2.2.1 (Media Cybernetics, Inc., Bethesda, MD; Fig. 1A). Binary cell masks were made to remove the extracellular area and to limit the colocalization analysis to a single cell. DIC and fluorescent images were used to create masks by tracing a cell's outline (Fig. 1B).

Chromatic Aberration Correction

Chromatic aberration is caused by inability of a lens to focus different wavelengths of light at one focal point, resulting in a blurred image with colored fringes around it. This can be avoided by using an apochromatic objective lens, but other sources like refractive index mismatch, a cover slip not parallel to the microscope slide, and slight optical path misalignment can also add chromatic aberration. To correct this error, we used polystyrene microspheres 1.0 µm in diameter (FluoSpheres F-13082; Invitrogen) as previously described [29]. The beads have excitation and emission spectra similar to the dual-color setup used in this study and should show 100% colocalization. These were diluted to a concentration of 1:1000, sonicated, air dried on a cover slip, and mounted in Vectashield mounting medium and sealed on a slide. Microspheres were imaged using the same acquisition parameters as for labeled cells, and the Image stacks were deconvolved. The bead centroids were calculated, and the distance between one bead's centroid in the green and in the red channel was calculated as shown by vector fields. Thus, 873 beads were analyzed in three dimensions, and average values of the measured distances were applied for translational shifting to correct the chromatic aberration. The same shift was applied to all the cellular data to measure the colocalization of the HLA receptors.

Colocalization Analysis

Colocalization was quantified using a distance-based image-processing approach introduced by Obara et al. [29] and Drelie Gelasca et al. [39]. Briefly, the colocalization algorithm uses MATLAB software (version R2010b with Image Processing Toolbox; MathWorks Inc., Natick, Massachusetts) and identifies punctate 3D blob-like features corresponding to fluorescent particles. The number and position of 3D blob-like receptors is, thus, determined in each red and green channel in three dimensions. To measure the colocalization of 3D blob-like particles in the dual-color fluorescence image with accuracy, their centroid positions were determined at subpixel resolution using weighted centroids. A matching procedure was performed for each receptor in the green channel to find its closest receptor in the red channel by correctly matching between the two vectors of intersecting positions, using the expected average radius of the circle of light r surrounding each centroid. For each receptor in one channel, the Euclidean distance to every receptor in the other channel was calculated. If the distance of the receptor pair is smaller than the maximum colocalization distance $d = 165$ nm, then the pair is considered colocalized. All the receptors are, thus, checked in the same way. The two receptors (one from the green and one from the red channel) were classified as noncolocalized if the maximum distance between their centroids exceeded a user-defined threshold of 165 nm. Results are shown as 3D scatterplots, with green and red asterisks for receptors in each channel and colocalized receptors encircled in blue (Fig. 1C). Intermolecular distances between colocalized receptor centroids are shown as color-coded 3D distance maps, with a histogram showing the distribution of colocalization distances (Fig. 1D). A minimum of six cells in three separate slides, with or without PG treatment, were analyzed ($n = 18$).

Statistical Analyses

Confocal 3D micrographs were analyzed by using a colocalization algorithm as described previously (Fig. 1, A–C). The total number of green and red HLA receptors was detected per single cell. The number of each HLA receptor (HLA-C, -E, and -G) present on ACH-3P and JEG-3 cells with or without PG treatment was estimated, analyzing each cell separately. Pearson correlation analysis and Student t-test, calculated with SigmaPlot v12.3 (Systat Software Inc., Bangalore, India), were employed to investigate statistically the relationships between the two HLA receptors and PG treatment in both ACH-3P and JEG-3 cells. Only those values with a $P < 0.05$ were considered significant.

RESULTS

Phenotyping of HLA Class I Molecules on Trophoblast Cell Lines

ACH-3P and JEG-3 cells showed expression of HLA-C, -E, and -G on the cell membrane. Expression of HLA-F was not detected at the cell surface of either JEG-3 or ACH-3P cells (Fig. 2A). The ACH-3P cells showed two peaks for HLA-G (Fig. 2A), representing two populations of cells, where extravillous cells are identified by the HLA-G-positive population and villous trophoblast cells by the HLA-G-negative population, as shown in Figure 2A.

Immunoblot Analysis of HLA Class I Proteins

HLA-G, -E, -C, and -F were detected in both cell lines (Fig. 2B). Comparatively, JEG-3 cells expressed more HLA proteins than ACH-3P cells. The results also indicated that the amount of protein expressed inside the cells reflects the amount of protein on the cell surface. In contrast, HLA-F was present in the cytoplasm but did not appear on the trophoblast cell surface. Results from alpha-tubulin show that equal amounts of total proteins were loaded from each cell line.

Surface Antigen Quantification

For quantification purposes, the value of isotype control antigen-binding capacity (ABC) was subtracted from the ABC of each antigen under study, giving specific antigen-binding capacity (SABC). SABC determines the number of primary mouse monoclonal antibodies per cell after corrections for background antibody equivalent.

Quantification analysis revealed that JEG-3 cells expressed significantly higher amounts of HLA-G molecules on the surface as compared to ACH-3P cells ($P < 0.005$), whereas there was no significant difference in the amount of HLA-E and -C molecules on the surface of both cell lines. The relative abundance of proteins on the surface of ACH-3P and JEG-3 cells is shown in Table 1.

Confocal Microscopy

Immunofluorescence-stained cells were imaged at single-cell level, and surface receptors were visualized separately at different wavelengths, appearing as green and red spots in the image (Fig. 3). The HLA class I-specific antibodies used in this study are highly specific and well characterized in the literature. The possibility of interaction of MEM-E/07 and L31 monoclonal antibodies with isoforms of HLA-B can be dismissed, since the primary trophoblast and human choriocarcinoma cell lines do not express HLA-B [40]. The negative control samples were stained with mouse IgG isotype and secondary antibodies and imaged using the image acquisition protocol described above, whereby no signals above background fluorescence are observed. This minimizes false-positive signals.

Confocal microscopic images of all HLA receptors tagged with antibodies appeared as masses of spherical, blurred spots over the cell surface. In each HLA pair under study, surface receptors were imaged separately at different wavelengths, resulting as green or red spots of uniform size laterally (xy), whereas in the axial (z) direction receptors appear as cigar shaped. In the HLA-G and -E study group, HLA-G molecules are seen as green spots and HLA-E molecules as red spots, while yellow/orange spots represent coexpressed HLA-G and -E molecules (Fig. 3, left panel). In the HLA-G and -C pair, green denotes HLA-G and red denotes HLA-C, whereas yellow/orange signifies closely associated HLA-G and -C receptors (Fig. 3, middle panel). In the case of the HLA-C/HLA-E pair, green represents HLA-E, red indicates HLA-C, and yellow/orange indicates coexpressed HLA-E and -C (Fig. 3, right panel). The single-cell images showed uniform distribution of all HLA receptors on the trophoblast cell membrane.

Colocalization Analysis

This colocalization study quantitatively characterizes the total number of HLA-C, -E, and -G receptors per cell and the number of colocalized HLA-G/HLA-E, HLA-G/HLA-C, and HLA-C/HLA-E receptor pairs per cell. Red and green receptors colocalized on the surface of individual cells using a threshold of 165 nm. Histograms peaked at 58 nm Euclidean colocalization distance (Fig. 1D). Data were also compared between PG-treated and untreated groups (Fig. 4, A and B, and Table 2).

The average relative ratio of HLA-G/HLA-E colocalization in untreated ACH-3P cells was 23% ± 3%, whereas PG treatment led to an increase of 30% ± 7%. JEG-3 cells showed a similar response to PG, with an increase from 20% ± 4% in untreated cells to 30% ± 8% in PG-treated cells. The data from HLA-G/HLA-C colocalization analysis showed very similar values between untreated and PG-treated ACH-3P cells (average value of 24% in both cases). In JEG-3 cells, PG treatment induced a slight decrease from 20% ± 7% to 18 % ± 4% in the average ratio of colocalized HLA-G/HLA-C molecules. In the ACH-3P cell line, the average ratio for HLA-

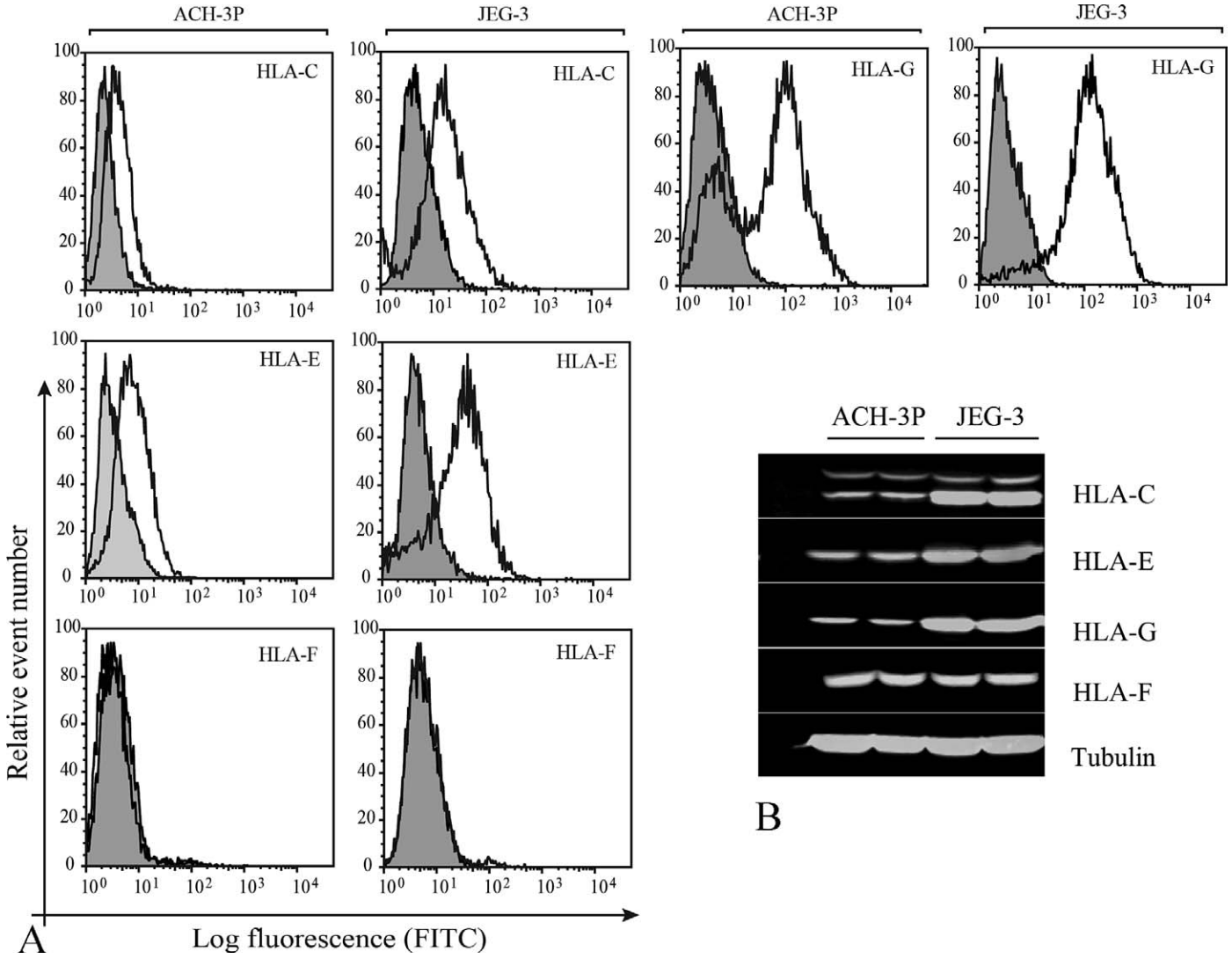

FIG. 2. Semiquantitative analysis of the expression of cell surface and total HLA-C, -E, -F, and -G in the trophoblast cell lines ACH-3P and JEG-3. **A**) Flow cytometry analysis showing HLA-C, -E, -F, and -G expression (empty histograms), displayed as mean fluorescence intensity, at the cell surface of ACH-3P and JEG-3 cells. Controls were performed by using an isotype-matched control antibody (gray-filled histograms). **B**) Western blot of ACH-3P and JEG-3 cells. An empty well on the left of each immunoblot was loaded with lysis and sample buffer only and served as the negative control. Tubulin was used as a loading control. A representative immunoblot of three independent experiments is shown.

E/HLA-C colocalization was 11% in both the PG-treated and untreated groups. In the JEG-3 cell line, the estimated ratio for colocalization was 22% in both treated and untreated subsets. Statistical analysis of colocalized HLA-G and -E molecules showed significant differences in untreated and PG-treated JEG-3 and ACH-3P cells. PG treatment did not significantly affect the colocalization ratios of the HLA-G/HLA-C and HLA-E/HLA-C pairs in either cell line.

TABLE 1. Relative receptor density and comparison of HLA-C, HLA-E, and HLA-G on the cell surface of ACH-3P and JEG-3 cells.

	Mean antigen density on cell surface		
Molecules	ACH-3P	JEG-3	*P* value[a]
HLA-C	3066 ± 1590	3347 ± 1621	0.84
HLA-E	7872 ± 2669	9473 ± 2590	0.49
HLA-G	16 799 ± 1700	30 581 ± 1900	0.0007

[a] Student *t*-test (unpaired).

Correlation Analysis for HLA Pairs

Strong linear correlation was observed between HLA receptor pairs irrespective of PG treatment, showing that an increase or decrease in the number of one HLA receptor has a similar effect on its partner, suggesting interdependence of cell surface-expressed HLA class I molecules (Fig. 5). All data were statistically significant ($P < 0.05$).

DISCUSSION

The human MHC class I genes HLA-G, -E, -F, and -C encode integral membrane glycoproteins that exhibit lateral mobility and, thus, have the potential to form physical interactions, including heterotypic associations. Unlike the classical HLA class Ia, HLA-A, -B, -C, the HLA class Ib are defined as nonclassical, and they are thought to play a role in regulation of immune and reproductive functions [41–47]. Previous studies on the physical association of HLA class I molecules have been hampered by the lack of reproducible and sensitive colocalization methods to detect and quantify antigen

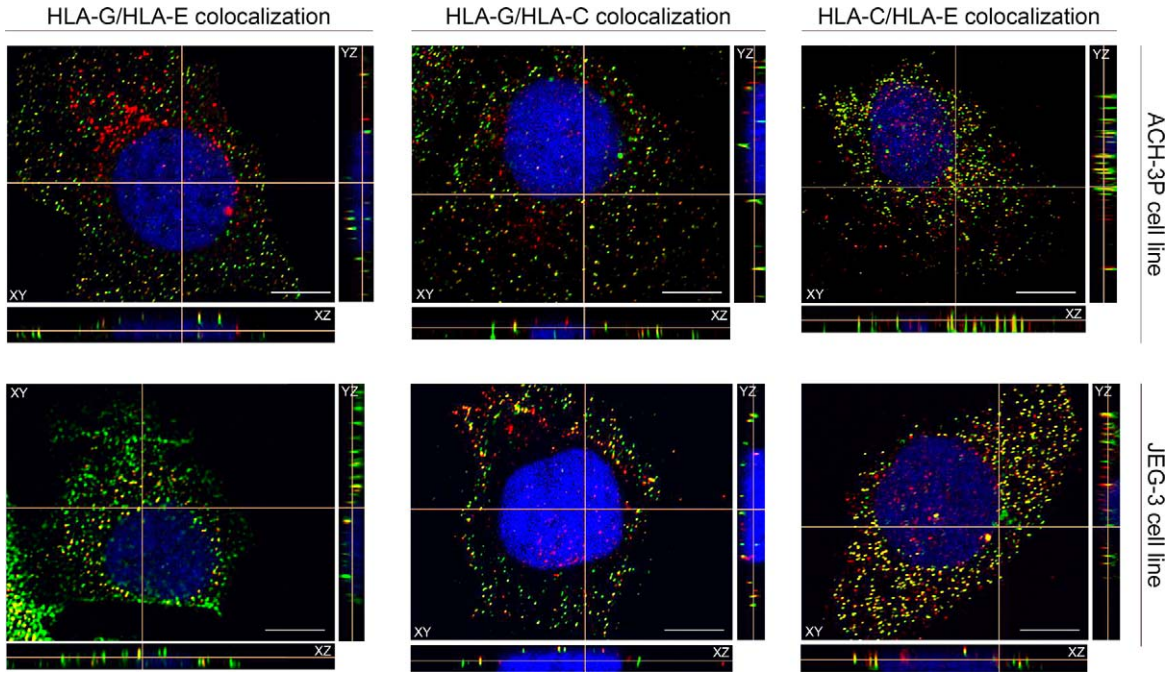

FIG. 3. Localization of HLA-C, -E, and -G on the cell surface of ACH-3P and JEG-3 cells, determined by confocal microscopy analysis. Green and red indicate pairings as follows: HLA-G (green)/HLA-E (red), HLA-G (green)/HLA-C (red), and HLA-C (red)/HLA-E (green). Yellow/orange fluorescence reveals the potential colocalization of two antigens. 3D images were acquired in stacks, with z-direction step size 0.14 μm. Single-plane section of z-stack is shown in three directions as *xy*, *yz*, and *zx*. The cutting planes of the cell section are indicated by gray/pale horizontal and vertical lines. A representative single cell from each HLA group is shown. Bar = 10 μm.

interaction. However, improved techniques for the detection of neighboring pairs of molecules have been developed. These developments have significantly enhanced the capacity to interpret data using either intact IgG or Fab antibody probes coupled with sensitive image-acquisition and analysis protocols [22, 28, 48]. We and others have previously reported self-associations of HLA class I molecules in lymphoid cells and their significance [49–51].

In this study, we have analyzed and quantified all the HLA class I molecules present on the surface of trophoblast cells; these are the extensively studied HLA-G and the less investigated HLA-F, -E, and -C subsets. We have shown that JEG-3 and ACH-3P cells express high levels of HLA-G and HLA-E. Quantification and Western blot analysis revealed that ACH-3P cells bore almost half the amounts of HLA-G present in JEG-3 cells. The existence of this disparity between the relative expression levels of HLA-G and -E in JEG-3 and ACH-3P cells can be explained by the presence of villous and EVT subpopulations in the ACH-3P cell line, as reported earlier [30]. A fluorescence microscopy study showed that the distribution patterns of HLA-G, -E, and -C are similar on the cell surface of both cell lines and are in agreement with a recent study of first-trimester invasive trophoblast cells [43], suggesting that both cell lines are good models to study HLA expression and function on human trophoblast cells. Several studies have shown that HLA class Ib molecules, which can interact with multiple receptors on the cell surface of immunocompetent cells, play an essential role during pregnancy in modulating the immune response. The formation of HLA-G and HLA-G homodimers has been shown to protect the cytotrophoblasts against cell lysis through direct interaction with the killer cell Ig-like receptor (KIR)2DL4 and with

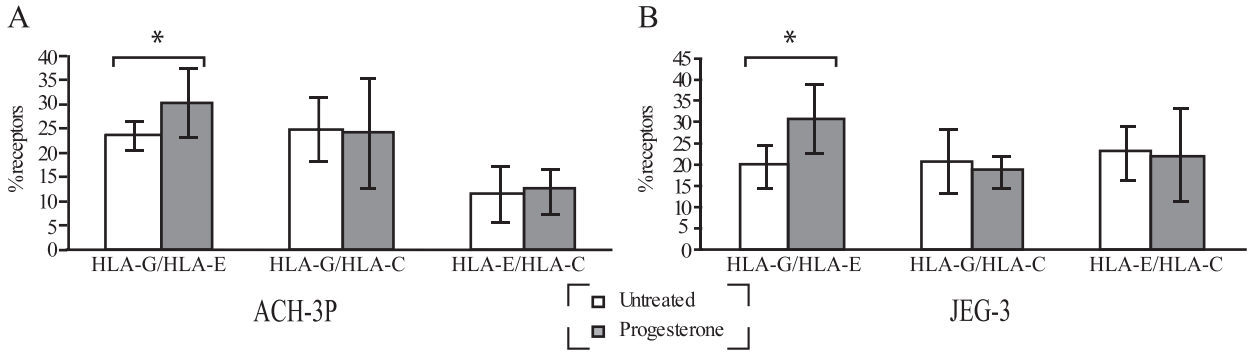

FIG. 4. Ratios of HLA receptor pairs, coexpressed on the cell surface of ACH-3P (**A**) and JEG-3 (**B**) cells, with and without PG treatment. Comparison of fractions of HLA-G/HLA-E colocalization, HLA-G/HLA-C colocalization, and HLA-E/HLA-C colocalization between untreated (white bar) and PG-treated (gray bar) cells. Each data point represents mean ± SD of three independent experiments. Data were statistically analyzed using an unpaired Student *t*-test. *Significant difference compared with untreated cells ($P < 0.05$).

TABLE 2. Percentages of colocalized HLA-G, HLA-E, and HLA-C molecules at the cell surface of ACH-3P and JEG-3 cells, with or without progesterone treatment.

Cell line	HLA Pairs	Treatment	Sample size (no. of cells)	Colocalization (%)[a]	*P* value[b]
ACH-3P	G/E	Untreated	18	23 ± 3	0.01*
		Progesterone	18	30 ± 7	
	G/C	Untreated	18	24 ± 6	0.63
		Progesterone	18	24 ± 11	
	C/E	Untreated	18	11 ± 6	0.75
		Progesterone	18	11 ± 5	
JEG-3	G/E	Untreated	18	20 ± 4	0.04*
		Progesterone	18	30 ± 8	
	G/C	Untreated	18	20 ± 7	0.52
		Progesterone	18	18 ± 4	
	C/E	Untreated	18	22 ± 6	0.97
		Progesterone	18	22 ± 11	

[a] Values represent percentages of detected colocalized spots; variances are the standard deviations calculated over the number of separate cells analyzed.
[b] Treated and untreated groups are compared by two-tailed unpaired Student *t*-test (*statistically significant results).

leukocyte Ig-like receptors (LILR)B1 and B2 (formerly, Ig-like transcripts [ILT] 2 and 4) [52–59].

HLA-E is a ligand for the CD94/NKG2 family of receptors expressed on NK cells and some $CD8^+$ T cell subsets [60, 61]. It has been postulated that HLA-E inhibits cell lysis mediated by $CD94/NKG2A^+$ NK cells [62]. On the other hand, the classical molecule HLA-C, detected on JEG-3 and ACH-3P, can interact with the NK inhibitory receptors KIR2DL1 and

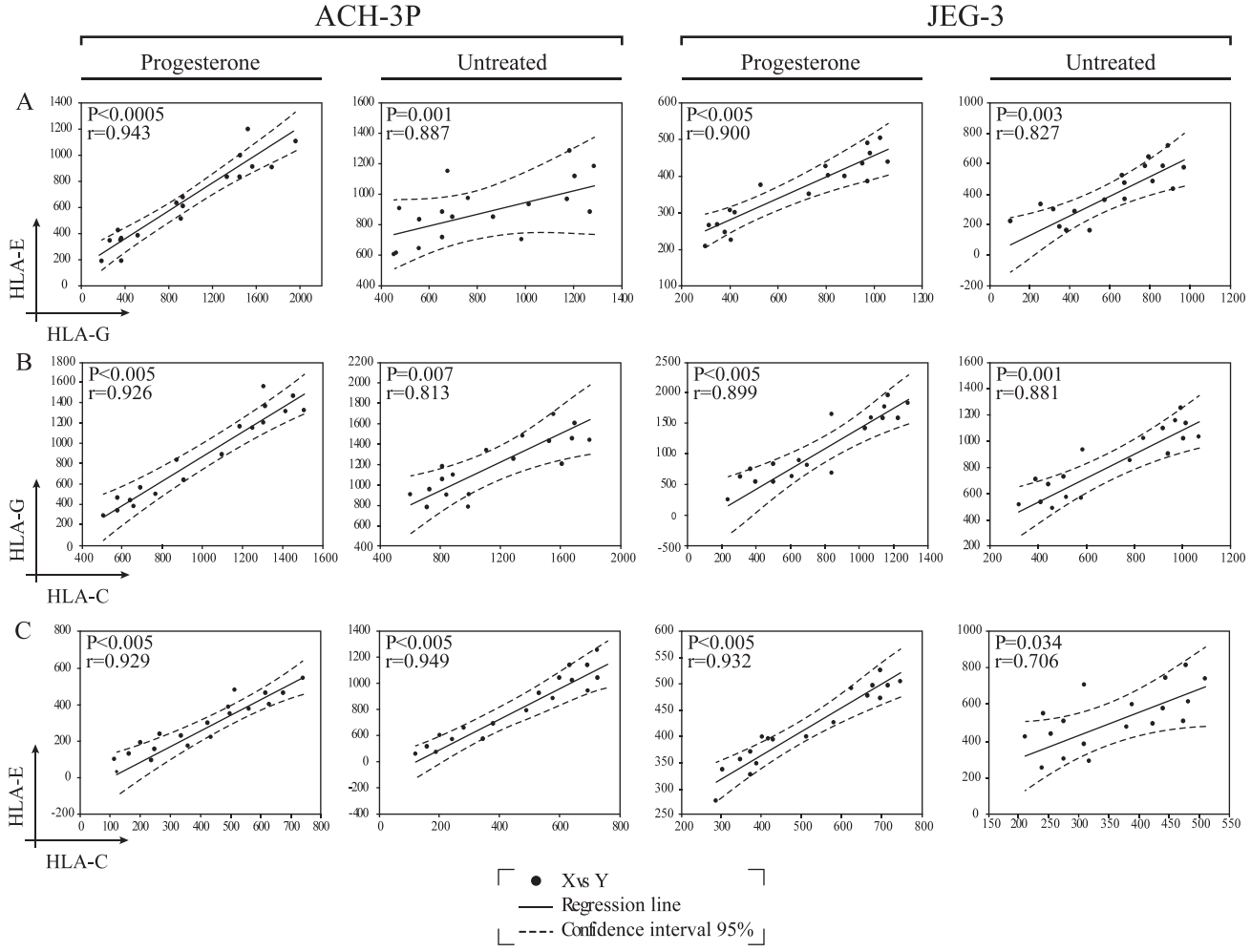

FIG. 5. Correlation analysis between number of HLA receptors expressed on the surface of ACH-3P and JEG-3 cells with and without PG treatment. Number of total HLA receptors per cell, as quantified by microscopic data analysis, has been used to estimate the correlation between each HLA pair under study. Scatter plots show the distribution of HLA-G (*x*-axis) versus HLA-E (*y*-axis) receptors (**A**), HLA-C (*x*-axis) versus HLA-G (*y*-axis) receptors (**B**), and HLA-C (*x*-axis) versus HLA-E (*y*-axis) receptors (**C**) for both cell lines under treated and untreated conditions. Data were analyzed using Pearson correlation, and the value of correlation coefficient *r* is shown in each graph. Straight lines represent linear regression, and curved lines are the 95% confidence interval. For all scatter plots, $P < 0.05$.

KIR2DL2 [63, 64], preventing NK killing during trophoblastic invasion of the decidua. This is in line with the postulate of the ''missing self'' hypothesis, in which NK cells display affinity and remove cells that do not express self HLA class I molecules [65].

Our data showed that neither JEG-3 nor ACH-3P cells express cell-surface HLA-F; expression was confined to the cytoplasm, as detected by Western blotting. This behavior of HLA-F expression by cell lines is in agreement with the findings of Nagamatsu et al. [66] that HLA-F is not expressed on the cell surface of cultured EVT of each trimester but is found in the cytoplasm. These data suggest that HLA-F might not be involved in cell-to-cell immunological interactions. These data also prove that both cell lines exhibit the human trophoblast phenotype.

In the present study, analysis of the heterotypic HLA associations of all class I molecules on the surface of JEG-3 and ACH-3P was undertaken using a microscopy approach with high measurement precision. We observed, for the first time, that potential physical heterotypic interactions exist between classical and nonclassical HLA class I molecules on the cell surface of human trophoblast cells. HLA-G and -E colocalization was detected on the trophoblast cell membrane of JEG-3 and ACH-3P cells. This substantiates the previous postulate that trophoblast HLA-E expression might be regulated by colocalization with HLA-G, where the average percentage of each HLA-G and -E receptor was calculated out of total colocalized receptors [67]. Similar ratios of HLA-G and -E colocalizations were observed previously by employing the latest bioimage informatics tools [29]. In this study, the ratios of receptor pair colocalizations were calculated by considering total colocalized molecules out of total red and green spots per cell. This calculation method is an improvement for the comparison between treated and untreated groups. We observe that the relative ratios of colocalized HLA-G/HLA-E molecules increase by 7%–10% in response to PG treatment in both study models. This finding is also in agreement with the observation that cell-surface expression of HLA-E is dependent upon the availability of a leader sequence from class Ia and HLA-G nonamers. Since HLA-E and -G can interact with the CD94/NKG2 and KIR2DL receptor family and the ILT2 and ILT4 receptors to promote or inhibit the NK and cytotoxic T lymphocyte activation [68, 69], HLA-E and -G colocalization might indicate that these two molecules work together, inhibiting NK cytotoxicity and activating NK cells to secrete cytokines. A consequence of the HLA-E and -G interaction is that the surge of cytokines released following association might also regulate placentation. Our data also suggest that PG can regulate the expression of this heterodimer, increasing its expression on the cell surface. These findings are in agreement with previous studies that have shown that PG upregulates the expression of HLA-G [70] and HLA-E [71] as individual molecules but not as heterotypic pairs. Our new data indicate that this upregulation contributes to the heterotypic association of HLA class I molecules. PG is essential for placentation and normal maintenance of pregnancy. It is first produced by the corpus luteum, then by the placenta itself [72], and can, thus, regulate the HLA class Ia expression and these heterotypic associations.

Though it is known that HLA-G, -E, and -C are expressed by invasive trophoblast cells as single membrane-bound molecules [43, 73], little is known regarding their heterotypic associations. In this study, the association of classical and nonclassical HLA molecules on the cell surface of trophoblast cells is described for the first time. We have observed that HLA-C molecules can form heterotypic associations with HLA-G and -E on the cell membrane of JEG-3 and ACH-3P cells. In contrast to HLA-G/HLA-E colocalized pairs, the colocalization of HLA-G/HLA-C and HLA-E/HLA-C remained unaffected in response to PG treatment. Given the structural similarity of HLA-E and -C molecules and their NK cell-inhibiting activities [5, 60, 74], it is not surprising that HLA subtypes form heterodimers on the cell surface of JEG-3 and ACH-3P cells. The fact that HLA-G and -E are coexpressed and have comparable functions during pregnancy has implications for understanding the way HLA-C and -G molecules work in synergy. Potentially, HLA-E could play an important role in modulating immune tolerance toward a successful pregnancy. We cannot disregard the possibility that this phenotype could be related to the origin of both cell lines, since both are derived from noninvasive trophoblast cells. Nonetheless, we also considered that in the course of trophoblast invasion the cells may change their phenotype, as previously shown [6]. This phenotypic modulation may regulate the local immune response during invasion and the implantation phase of embryonic development. This research provides a new, sensitive, object-based colocalization technique that is able to detect and quantify fluorescent antibody-tagged isotropic particles in 3D cell images.

In summary, our colocalization technique enabled us to quantify and detect subtle differences in HLA surface receptor distribution. The trophoblast cell lines ACH-3P and JEG-3 serve as a good study model to develop this approach and to investigate base line information on potential HLA class I molecule associations. We conclude that by applying a sensitive, sparse colocalization quantification method, we have found that HLA-G, -C, and -E molecules colocalize with each other, forming preferential associations on the cell membranes of trophoblast-derived cells. There appear to be favored combinations of certain HLA class I sub-sets, and these may enhance cell-to-cell apposition. It is reasonable to assume that this is likely to be an immune-effector mechanism that protects the fetus by promoting trophoblast-uterine effector cell interactions mediated by class I heterotypic clusters, thus enhancing the intracellular signaling to allow successful placentation.

ACKNOWLEDGMENT

We thank Dr. G. Desoye for providing the ACH-3P cell line, Professor I.L. Sargent for providing the JEG-3 cell line, and Dr. D. Geraghty for providing the anti-HLA-F clone 3D11.

REFERENCES

1. King A, Boocock C, Sharkey AM, Gardner L, Beretta A, Siccardi AG, Loke YW. Evidence for the expression of HLAA-C class I mRNA and protein by human first trimester trophoblast. J Immunol 1996; 156: 2068–2076.
2. Jurisicova A, Casper RF, MacLusky NJ, Mills GB, Librach CL. HLA-G expression during preimplantation human embryo development. Proc Natl Acad Sci U S A 1996; 93:161–165.
3. Chumbley G, King A, Holmes N, Loke YW. In situ hybridization and northern blot demonstration of HLA-G mRNA in human trophoblast populations by locus-specific oligonucleotide. Hum Immunol 1993; 37: 17–22.
4. Ellis SA, Palmer MS, McMichael AJ. Human trophoblast and the choriocarcinoma cell line BeWo express a truncated HLA Class I molecule. J Immunol 1990; 144:731–735.
5. King A, Allan DS, Bowen M, Powis SJ, Joseph S, Verma S, Hiby SE, McMichael AJ, Loke YW, Braud VM. HLA-E is expressed on trophoblast and interacts with CD94/NKG2 receptors on decidual NK cells. Eur J Immunol 2000; 30:1623–1631.
6. Ishitani A, Sageshima N, Lee N, Dorofeeva N, Hatake K, Marquardt H, Geraghty DE. Protein expression and peptide binding suggest unique and

interacting functional roles for HLA-E, F, and G in maternal-placental immune recognition. J Immunol 2003; 171:1376–1384.
7. Shobu T, Sageshima N, Tokui H, Omura M, Saito K, Nagatsuka Y, Nakanishi M, Hayashi Y, Hatake K, Ishitani A. The surface expression of HLA-F on decidual trophoblasts increases from mid to term gestation. J Reprod Immunol 2006; 72:18–32.
8. Karre K. NK cells, MHC class I molecules and the missing self. Scand J Immunol 2002; 55:221–228.
9. Favier B, LeMaoult J, Rouas-Freiss N, Moreau P, Menier C, Carosella ED. Research on HLA-G: an update. Tissue Antigens 2007; 69:207–211.
10. Sargent IL. Does 'soluble' HLA-G really exist? Another twist to the tale. Mol Hum Reprod 2005; 11:695–698.
11. Bainbridge D, Ellis S, Le Bouteiller P, Sargent I. HLA-G remains a mystery. Trends Immunol 2001; 22:548–552.
12. Yao YQ, Barlow DH, Sargent IL. Differential expression of alternatively spliced transcripts of HLA-G in human preimplantation embryos and inner cell masses. J Immunol 2005; 175:8379–8385.
13. Tripathi P, Naik S, Agrawal S. Role of HLA-G, HLA-E and KIR2DL4 in pregnancy. Int J Hum Genet 2007; 7:219–233.
14. Kaiser BK, Barahmand-Pour F, Paulsene W, Medley S, Geraghty DE, Strong RK. Interactions between NKG2x immunoreceptors and HLA-E ligands display overlapping affinities and thermodynamics. J Immunol 2005; 174:2878–2884.
15. Lepin EJ, Bastin JM, Allan DS, Roncador G, Braud VM, Mason DY, van der Merwe PA, McMichael AJ, Bell JI, Powis SH, O'Callaghan CA. Functional characterization of HLA-F and binding of HLA-F tetramers to ILT2 and ILT4 receptors. Eur J Immunol 2000; 30:3552–3561.
16. Wainwright SD, Biro PA, Holmes CH. HLA-F is a predominantly empty, intracellular, TAP-associated MHC class Ib protein with a restricted expression pattern. J Immunol 2000; 164:319–328.
17. Lee N, Geraghty DE. HLA-F surface expression on B cell and monocyte cell lines is partially independent from tapasin and completely independent from TAP. J Immunol 2003; 171:5264–5271.
18. Heisenberg W, Eckart C, Hoyt FC. The Physical Principles of the Quantum Theory. Chicago: The University of Chicago Press; 1930.
19. Bobroff N. Position measurement with a resolution and noise-limited instrument. Rev Sci Instrum 1986; 57:1152–1157.
20. Gross D, Webb WW. Cell surface clustering and mobility of the liganded LDL receptor measured by digital video fluorescence microscopy. In: Loew LM (ed.), Spectroscopic Membrane Probes, vol. 2. Boca Raton, FL: CRC Press; 1988:9–45.
21. Anderson CM, Georgiou GN, Morrison IE, Stevenson GV, Cherry RJ. Tracking of cell surface receptors by fluorescence digital imaging microscopy using a charge-coupled device camera. Low-density lipoprotein and influenza virus receptor mobility at 4 degrees C. J Cell Sci 1992; 101(pt 2):415–425.
22. Cherry RJ, Wilson KM, Triantafilou K, O'Toole P, Morrison IE, Smith PR, Fernandez N. Detection of dimers of dimers of human leukocyte antigen (HLA)-DR on the surface of living cells by single-particle fluorescence imaging. J Cell Biol 1998; 140:71–79.
23. Thompson RE, Larson DR, Webb WW. Precise nanometer localization analysis for individual fluorescent probes. Biophys J 2002; 82:2775–2783.
24. Betzig E, Patterson GH, Sougrat R, Lindwasser OW, Olenych S, Bonifacino JS, Davidson MW, Lippincott-Schwartz J, Hess HF. Imaging intracellular fluorescent proteins at nanometer resolution. Science 2006; 313:1642–1645.
25. Yildiz A, Forkey JN, McKinney SA, Ha T, Goldman YE, Selvin PR. Myosin V walks hand-over-hand: single fluorophore imaging with 1.5-nm localization. Science 2003; 300:2061–2065.
26. Pertsinidis A, Zhang Y, Chu S. Subnanometre single-molecule localization, registration and distance measurements. Nature 2010; 466:647–651.
27. Schermelleh L, Heintzmann R, Leonhardt H. A guide to super-resolution fluorescence microscopy. J Cell Biol 2010; 190:165–175.
28. Morrison IE, Karakikes I, Barber RE, Fernandez N, Cherry RJ. Detecting and quantifying colocalization of cell surface molecules by single particle fluorescence imaging. Biophys J 2003; 85:4110–4121.
29. Obara B, Jabeen A, Fernandez N, Laissue PP. A novel method for quantified, superresolved, three-dimensional colocalisation of isotropic, fluorescent particles. Histochem Cell Biol 2013; 139:391–402.
30. Hiden U, Wadsack C, Prutsch N, Gauster M, Weiss U, Frank HG, Schmitz U, Fast-Hirsch C, Hengstschlager M, Potgens A, Ruben A, Knofler M, et al. The first trimester human trophoblast cell line ACH-3P: a novel tool to study autocrine/paracrine regulatory loops of human trophoblast subpopulations—TNF-alpha stimulates MMP15 expression. BMC Dev Biol 2007; 7:137.
31. Menier C, Saez B, Horejsi V, Martinozzi S, Krawice-Radanne I, Bruel S, Le Danff C, Reboul M, Hilgert I, Rabreau M, Larrad ML, Pla M, et al. Characterization of monoclonal antibodies recognizing HLA-G or HLA-E: new tools to analyze the expression of nonclassical HLA class I molecules. Hum Immunol 2003; 64:315–326.
32. Palmisano GL, Contardi E, Morabito A, Gargaglione V, Ferrara GB, Pistillo MP. HLA-E surface expression is independent of the availability of HLA class I signal sequence-derived peptides in human tumor cell lines. Hum Immunol 2005; 66:1–12.
33. Zhao L, Teklemariam T, Hantash BM. Reassessment of HLA-G isoform specificity of MEM-G/9 and 4H84 monoclonal antibodies. Tissue Antigens 2012; 80:231–238.
34. Setini A, Beretta A, De Santis C, Meneveri R, Martayan A, Mazzilli MC, Appella E, Siccardi AG, Natali PG, Giacomini P. Distinctive features of the alpha 1-domain alpha helix of HLA-C heavy chains free of beta 2-microglobulin. Hum Immunol 1996; 46:69–81.
35. Coupel S, Moreau A, Hamidou M, Horejsi V, Soulillou JP, Charreau B. Expression and release of soluble HLA-E is an immunoregulatory feature of endothelial cell activation. Blood 2007; 109:2806–2814.
36. Shaikly V, Shakhawat A, Withey A, Morrison I, Taranissi M, Dealtry GB, Jabeen A, Cherry R, Fernandez N. Cell bio-imaging reveals co-expression of HLA-G and HLA-E in human preimplantation embryos. Reprod Biomed Online 2010; 20:223–233.
37. Thevenaz P, Ruttimann UE, Unser M. A pyramid approach to subpixel registration based on intensity. IEEE Trans Image Process 1998; 7:27–41.
38. Rasband WS. Imagej. Bethesda, MD: National Institutes of Health; 1997.
39. Drelie Gelasca E, Obara B, Fedorov D, Kvilekval K, Manjunath B. A biosegmentation benchmark for evaluation of bioimage analysis methods. BMC Bioinformatics 2009; 10:368.
40. Apps R, Murphy SP, Fernando R, Gardner L, Ahad T, Moffett A. Human leucocyte antigen (HLA) expression of primary trophoblast cells and placental cell lines, determined using single antigen beads to characterize allotype specificities of anti-HLA antibodies. Immunology 2009; 127: 26–39.
41. Hemberger M. Health during pregnancy and beyond: fetal trophoblast cells as chief co-ordinators of intrauterine growth and reproductive success. Ann Med 2012; 44:325–337.
42. Hutter H, Hammer A, Blaschitz A, Hartmann M, Ebbesen P, Dohr G, Ziegler A, Uchanska-Ziegler B. Expression of HLA class I molecules in human first trimester and term placenta trophoblast. Cell Tissue Res 1996; 286:439–447.
43. Juch H, Blaschitz A, Dohr G, Hutter H. HLA class I expression in the human placenta. Wien Med Wochenschr 2012; 162:196–200.
44. Thellin O, Coumans B, Zorzi W, Igout A, Heinen E. Tolerance to the foeto-placental 'graft': ten ways to support a child for nine months. Curr Opin Immunol 2000; 12:731–737.
45. Weetman AP. The immunology of pregnancy. Thyroid 1999; 9:643–646.
46. Rodgers JR, Cook RG. MHC class Ib molecules bridge innate and acquired immunity. Nat Rev Immunol 2005; 5:459–471.
47. Sprinks MT, Sellens MH, Dealtry GB, Fernandez N. Preimplantation mouse embryos express Mhc class I genes before the first cleavage division. Immunogenetics 1993; 38:35–40.
48. Karakikes I, Morrison IE, O'Toole P, Metodieva G, Navarrete CV, Gomez J, Miranda-Sayago JM, Cherry RJ, Metodiev M, Fernandez N. Interaction of HLA-DR and CD74 at the cell surface of antigen-presenting cells by single particle image analysis. FASEB J 2012; 26:4886–4896.
49. Matko J, Bushkin Y, Wei T, Edidin M. Clustering of class I HLA molecules on the surfaces of activated and transformed human cells. J Immunol 1994; 152:3353–3360.
50. Smith PR, Morrison IE, Wilson KM, Fernandez N, Cherry RJ. Anomalous diffusion of major histocompatibility complex class I molecules on HeLa cells determined by single particle tracking. Biophys J 1999; 76: 3331–3344.
51. Chakrabarti A, Matko J, Rahman NA, Barisas BG, Edidin M. Self-association of class I major histocompatibility complex molecules in liposome and cell surface membranes. Biochemistry 1992; 31:7182–7189.
52. Rouas-Freiss N, Goncalves RM, Menier C, Dausset J, Carosella ED. Direct evidence to support the role of HLA-G in protecting the fetus from maternal uterine natural killer cytolysis. Proc Natl Acad Sci U S A 1997; 94:11520–11525.
53. Pazmany L, Mandelboim O, Vales-Gomez M, Davis DM, Reyburn HT, Strominger JL. Protection from natural killer cell-mediated lysis by HLA-G expression on target cells. Science 1996; 274:792–795.
54. Perez-Villar JJ, Melero I, Navarro F, Carretero M, Bellon T, Llano M, Colonna M, Geraghty DE, Lopez-Botet M. The CD94/NKG2-A inhibitory receptor complex is involved in natural killer cell-mediated recognition of cells expressing HLA-G1. J Immunol 1997; 158:5736–5743.
55. Shiroishi M, Kuroki K, Ose T, Rasubala L, Shiratori I, Arase H, Tsumoto K, Kumagai I, Kohda D, Maenaka K. Efficient leukocyte Ig-like receptor

signaling and crystal structure of disulfide-linked HLA-G dimer. J Biol Chem 2006; 281:10439–10447.
56. Hviid TV. HLA-G in human reproduction: aspects of genetics, function and pregnancy complications. Hum Reprod Update 2006; 12:209–232.
57. Sanders SK, Giblin PA, Kavathas P. Cell-cell adhesion mediated by CD8 and human histocompatibility leukocyte antigen G, a nonclassical major histocompatibility complex class 1 molecule on cytotrophoblasts. J Exp Med 1991; 174:737–740.
58. Apps R, Gardner L, Sharkey AM, Holmes N, Moffett A. A homodimeric complex of HLA-G on normal trophoblast cells modulates antigen-presenting cells via LILRB1. Eur J Immunol 2007; 37:1924–1937.
59. Li C, Houser BL, Nicotra ML, Strominger JL. HLA-G homodimer-induced cytokine secretion through HLA-G receptors on human decidual macrophages and natural killer cells. Proc Natl Acad Sci U S A 2009; 106: 5767–5772.
60. Braud VM, Allan DS, O'Callaghan CA, Soderstrom K, D'Andrea A, Ogg GS, Lazetic S, Young NT, Bell JI, Phillips JH, Lanier LL, McMichael AJ. HLA-E binds to natural killer cell receptors CD94/NKG2A, B and C. Nature 1998; 391:795–799.
61. Kaiser BK, Pizarro JC, Kerns J, Strong RK. Structural basis for NKG2A/CD94 recognition of HLA-E. Proc Natl Acad Sci U S A 2008; 105: 6696–6701.
62. Lee N, Llano M, Carretero M, Ishitani A, Navarro F, Lopez-Botet M, Geraghty DE. HLA-E is a major ligand for the natural killer inhibitory receptor CD94/NKG2A. Proc Natl Acad Sci U S A 1998; 95:5199–5204.
63. Vales-Gomez M, Reyburn HT, Mandelboim M, Strominger JL. Kinetics of interaction of HLA-C ligands with natural killer cell inhibitory receptors. Immunity 1998; 9:337–344.
64. Fan QR, Long EO, Wiley DC. A disulfide-linked natural killer cell receptor dimer has higher affinity for HLA-C than wild-type monomer. Eur J Immunol 2000; 30:2692–2697.
65. Ljunggren HG, Karre K. In search of the 'missing self': MHC molecules and NK cell recognition. Immunol Today 1990; 11:237–244.
66. Nagamatsu T, Fujii T, Matsumoto J, Yamashita T, Kozuma S, Taketani Y. Human leukocyte antigen F protein is expressed in the extra-villous trophoblasts but not on the cell surface of them. Am J Reprod Immunol 2006; 56:172–177.
67. Shaikly VR, Morrison IE, Taranissi M, Noble CV, Withey AD, Cherry RJ, Blois SM, Fernandez N. Analysis of HLA-G in maternal plasma, follicular fluid, and preimplantation embryos reveal an asymmetric pattern of expression. J Immunol 2008; 180:4330–4337.
68. Parham P. MHC class I molecules and KIRs in human history, health and survival. Nat Rev Immunol 2005; 5:201–214.
69. Shiroishi M, Tsumoto K, Amano K, Shirakihara Y, Colonna M, Braud VM, Allan DS, Makadzange A, Rowland-Jones S, Willcox B, Jones EY, van der Merwe PA, et al. Human inhibitory receptors Ig-like transcript 2 (ILT2) and ILT4 compete with CD8 for MHC class I binding and bind preferentially to HLA-G. Proc Natl Acad Sci U S A 2003; 100:8856–8861.
70. Yie SM, Li LH, Li GM, Xiao R, Librach CL. Progesterone enhances HLA-G gene expression in JEG-3 choriocarcinoma cells and human cytotrophoblasts in vitro. Hum Reprod 2006; 21:46–51.
71. Huang Z, Hyodo H, Fujii T, Nagamatsu T, Matsumoto J, Kawana K, Yamashita T, Yasugi T, Kozuma S, Taketani Y. Effect of progesterone on HLA-E gene expression in JEG-3 choriocarcinoma cell line. Am J Reprod Immunol 2009; 61:221–226.
72. Tuckey RC. Progesterone synthesis by the human placenta. Placenta 2005; 26:273–281.
73. Riley JK. Trophoblast immune receptors in maternal-fetal tolerance. Immunol Invest 2008; 37:395–426.
74. Lee N, Goodlett DR, Ishitani A, Marquardt H, Geraghty DE. HLA-E surface expression depends on binding of TAP-dependent peptides derived from certain HLA class I signal sequences. J Immunol 1998; 160: 4951–4960.